und falls x, $\tau_{ad} = \text{const}$ (für konst. Unterlagentemperatur):

$$n/t_K \sim \dot{N}^2 \sim u^2, \qquad (2)$$

u = Aufdampfgeschwindigkeit der Keimsubstanz.

Nach (2) ist also ein quadratischer Anstieg der (auf gleiche Aufdampfzeiten der Keimsubstanz bezogenen) Kristallitzahldichte mit der Aufdampfgeschwindigkeit der Keimsubstanz (u) zu erwarten. Die Meßwerte zeigen tatsächlich eine stark ansteigende Tendenz der n/t_K-Werte mit u. Ein genauerer Vergleich ist jedoch wegen der erheblichen Streuung der Meßwerte nicht möglich.

Nimmt man für das LiF-Molekül einen Wirkungsdurchmesser von $3\,d$ ($d = 2{,}01$ Å) an, so erhält man für die mittlere freie Weglänge λ im zweidimensionalen Gas:

$$\lambda = \frac{1}{3\,d\,\tau_{ad}\,\dot{N}};$$

damit ergibt sich:

$$n/t_K = \dot{N} \cdot x/\lambda = 6{,}03 \cdot 10^{-4}\, x\, \tau_{ad}\, \dot{N}^2. \qquad (2\,a)$$

Setzt man in Gl. (2 a) den Meßpunkt ($u = 0{,}27$ Å/sec $\triangleq 2{,}35 \cdot 10^6$ LiF-Moleküle/μ^2 sec; $n/t_K = 0{,}26$ Kristallite/μ^2 sec) ein, so erhält man:

$$x\,\tau_{ad} = 7{,}82 \cdot 10^{-11} \quad (x \text{ gerechnet in } \mu). \qquad (3)$$

Nimmt man als Minimum der Reichweite eines LiF-Moleküls auf der KCl-Spaltfläche einmal 5 Å an, so kann die mittlere Verweilzeit eines einzelnen LiF-Moleküls nach Gl. (3) nicht über etwa $1{,}5 \cdot 10^{-7}$ sec hinausgehen.

Die Untersuchungen wurden im Institut für Angewandte Physik der Universität Hamburg durchgeführt. Dem Leiter des Instituts, Herrn Prof. Dr. H. Raether, danke ich für die Anregung und Förderung der Arbeit.

Dem Leiter der Virusabteilung des Tropeninstituts in Hamburg, Herrn Dr. Peters, und seinem Mitarbeiter, Herrn Giese, danke ich für die Hilfe bei der Herstellung von elektronenmikroskopischen Aufnahmen mit dem Siemens-Elmiskop I.

Ebenfalls habe ich der Deutschen Forschungsgemeinschaft zu danken, die mir zur Durchführung der Untersuchungen ein Interferenzmikroskop (Multimi) überließ.

Conductivity of Grown Germanium-Bicrystals

By H. F. Mataré *, B. Reed and O. A. Weinreich

Central Research Laboratories, Sylvania Electric Products Inc., Bayside, New York

(Z. Naturforschg. **14 a**, 281—284 [1959]; eingegangen am 10. November 1958)

Measurements of the grain boundary conduction in Ge-bicrystals grown from material of widely different impurity ranges show sheet resistivities of .003 to .01 ohm-cm for an assumed grain boundary layer width of 100 Å. This value is practically constant throughout a temperature range from 2 °K to 300 °K if leakage currents through the bulk are kept small by the use of junction contacts. This and the linear I—V characteristic suggest that the conductivity mechanism is dominated by the free orbitals and their overlapping wave functions in the internal surface layer.

Grain boundaries in germanium have been found to act like p-type material [1]. In n-type germanium, current flow perpendicular to the boundary shows the symmetrical rectifying characteristic of an n-p-n structure [1]. In p-type germanium, measurements of the photovoltage have the polarity corresponding to a p-p$^+$-p structure [2]. Tweet [3] has observed current flow in gold-doped germanium-bicrystals.

The present experiments were performed on bicrystals grown with (100) seeds tilted symmetrically about the (010) axis at angles of 10 – 25 degrees [4]. In order to observe conduction in the grain boundary sheet, it is necessary to negate the parallel bulk conduction by either low temperature or the use of rectifying contacts to the bulk [5]. The conduction of the sheet does not seem to be influenced by the nature of the contacts at low voltages. Within the temperature range over which the bulk resistance can be neglected, current flow in the grain boundary seems to be essentially independent of temperature.

A typical case of a comparison of the resistivity vs $1/T$ $(^\circ\text{K})^{-1}$ of a monocrystal and a bicrystal sheet is shown in Fig. 1. The bicrystal interface shows clearly a departure from the usual increase in resistivity towards lower temperatures, starting at 10 °K.

The ϱ-value at which the split occurs depends also on the bulk resistivity. The resistivity of the grain

* Now: Te Ka De-Semiconductor Div., Nürnberg/Germany.

[1] W. Taylor, N. Odell and N. Y. Fan, Phys. Rev. **88**, 867 [1952].

[2] O. A. Weinreich, H. F. Mataré and B. Reed, Enlarged Abstract 58, Electrochemical Society Meeting—Washington, D. C., May 12—16, 1957.

[3] G. Tweet, Phys. Rev. **99**, 1182 [1955].

[4] H. F. Mataré and H. H. R. Wegener, Z. Phys. **148**, 631 [1957].

[5] H. F. Mataré, B. Reed and O. A. Weinreich, Bull. Amer. Phys. Soc. **3** (D 12), 29 [1958].

* Fig. 2 on p. 280 b.

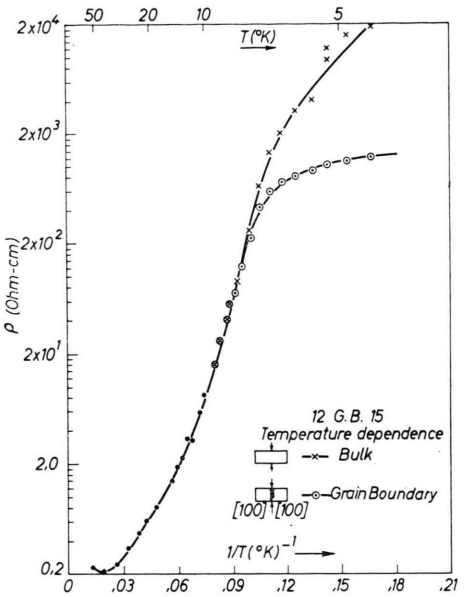

Fig. 1. Resistivity versus reciprocal absolute temperature of a monocrystal and a grain boundary sheet in a grown germanium bicrystal.

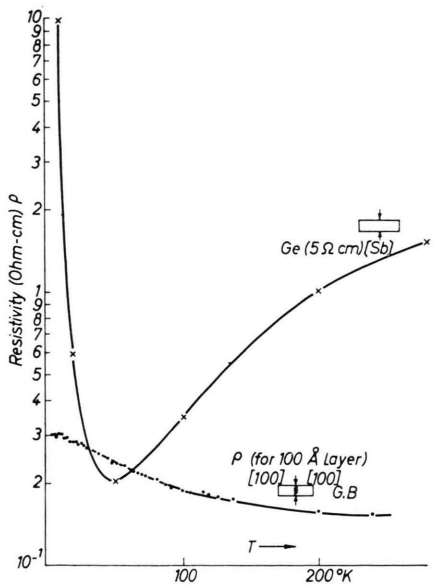

Fig. 3. Resistivity as a function of absolute temperature for a wide temperature range (20 °K—300 °K) for a Ge-monocrystal (5 Ohm cm, doped with Sb) and a Ge-bicrystal interface with indium contacts.

boundary sheet is calculated using a sheet-width-value of 100 Å. This value has been deduced as most propable mechanical width from one probe potential measurements and electron-microscope-pictures of etched bicrystal surfaces, (Fig. 2*).

In Fig. 3 the resistivities are plotted for the higher temperature range. Here also marked difference in temperature behavior of the grain boundary sheet and a monocrystal is apparent. Even at higher temperature, the slope of the $\varrho(T)$ curve for the bicrystal remains negative. (The plotted monocrystal did not belong to the bicrystal sides, which explains the difference in absolute ϱ-value.) While the contacts in both cases, Fig. 1 and Fig. 3, are ohmic in nature (soldered contacts), non-ohmic or alloyed contacts (indium on n-type Ge) may be used in order to yield a low contact potential to the p-type grain boundary and to form a blocking layer to the n-type bulk crystal. In this way, only the leakage

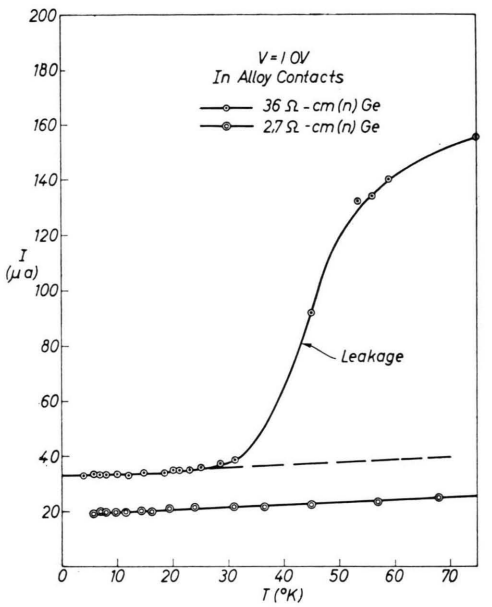

Fig. 4. Sheet conductance versus absolute temperature for two different germanium bicrystals with very different doping ranges. In the high resistivity case the junction leakage takes over in the higher temperature range.

current from the side of the sample, which works in the blocking direction defines the parallel current loss. The better the junction, or the lower the leakage, the more preponderant is the sheet in the current voltage and current temperature behavior.

In Fig. 4 two cases of sheet current vs T (°K) are drawn: one for a near intrinsic bicrystal (36 ohm-cm), one for low ohmic material (2.7 ohm-cm), both Sb doped. The difference is that for the intrinsic material the junction leakage current is high enough at 30 °K to take over, while for a better junction quality the sheet current is predominant for tem-

peratures in excess of 70 °K. Measurements at these crystals show that at liquid nitrogen temperature the sheet conductance is still clearly predominant. It is important to note that this material is not gold doped [3]. As Fig. 4 shows, there is a very small activation energy for the boundary sheet conduction. This behavior is also characteristic of bulk conductivity in highly doped material. The I – V characteristic at liquid helium temperature is linear for all samples at low voltages. For both n- and p-type germanium of a few ohm-cm resistivity, the departure from linearity is due to breakdown by field excitation of deionized impurities. In intrinsic samples and samples doped with 10^{16} Cu atoms per cc, the characteristics maintain their linearity to fields of at least 40 volts/cm.

Sample No.	ϱ (bulk) $T = 300$°K (ohm-cm)	Type	N Impurity (atoms/cc) approx.	Type	ϱ (grain boundary) $T = 4.2$°K (100Å)
17	4	n	10^{15}	Sb	0.0036
6	2.7	n	10^{15}	Sb	0.0075
9	1.75	p	10^{15}	Ga	0.0082
11	1.1	p	10^{15}	Ga	0.0102
12	1.1	p	10^{15}	Ga	0.0112
7	1.3	n	10^{15}	Sb	0.0078
3	5	n	3.10^{14}	Sb	0.0036
35	30		intrinsic		0.0056
42	1.6	n	10^{15}	Sb	0.0051
29	36		intrinsic		0.0041
31	4	p	10^{15}	Ga	0.0112
35	27		intrinsic		0.0136
27			10^{16}	Cu	0.0029
15			10^{16}	Cu	0.0037

$\bar{\varrho} = 0.007 \pm 5 \cdot 10^{-3}$.

Table 1.

In Table 1 we have compiled a number of Ge bicrystal samples with different doping, bulk resistivity and type.

The grain boundary sheet conductance has a mean value of $0.007 \pm 5 \cdot 10^{-3}$ ohm-cm and seems very independent from the wide variety of impurity types and concentrations, either grown-in or diffused-in. Due to the small dependence on impurities, it is believed that the grain boundary conduction is due to surface states arising from the dangling bonds at the grain boundary interface [6].

In a grain boundary structure, the misfit between neighboring atoms ($10^{14} - 10^{15}$ cm^{-2}) prevents the sharing of electrons by covalent bonds in a tetragonal arrangement about the individual atom. Most of the electrons will still be shared by hybrid orbital bonding with neighboring atoms in a higher energy situation. This high energy situation can be reduced by two atoms sharing a free electron which represents an unneutralized charge. Due to electrostatic repulsion between bound electrons, the minimum energy situation occurs when only a small fraction ($10^{11} - 10^{12}$ cm^{-2}) of the bonds are satisfied. These electrons are neutralized by free holes and ionized donors. Due to the independence of the grain boundary conduction from impurities, it seems that the filling factor for grain boundary states must depend solely on orientation of the two crystals.

The regular arrangement of edge dislocation pipes, equidistant at $D = a/2 \sin \Theta$- (a = lattice constant, $\Theta = 2 \times$ tilt angle) intervals in the symmetric case will create overlapping space charge cylinders. Their radii are given by:

$$R = [f/D\,\pi\,(N_d - N_a)]^{1/2}, \qquad (1)$$

$D = a/2 \sin \Theta$, N_d and N_a = donor, respectively acceptor densities. f is the fraction of sites that are full. Assuming this to be a FERMI function [7]:

$$f = \frac{1}{1+\exp[\underbrace{(E_d - E_F)}_{-\Delta E}/kT]} \qquad (2)$$

(E_d bound level, E_F FERMI level, T abs. temperature, k BOLTZMANN constant)

with the dangling bond levels E_d located slightly below the FERMI level at room temperature (ΔE small), f can be assumed in the order of 1/10. For a dislocation acceptor level of 0.225 eV below the conduction band, as measured in deformed samples (statistically distributed dislocation pipes), R is of the order of magnitude of 10^4 Å or $2 \cdot 10^3$ lattice constants. This is roughly 4 times the mean spacing between excess donors for $N_d - N_a = 10^{15}$ cm^{-3} in the bulk. The spacing of electrons in the dangling bond levels is $S = D/f \approx 40$ Å. Therefore, it follows that $S \ll R$ or the space charge cylinders are overlapping! Thus, the electrical width of the grain boundary plane is of the order of magnitude of the inversion layers at both sides adjacent to the n-type monocrystals.

With the filling factor $f = 1/10$ and an assumed width of the disturbed layer of 10^2 Å to 10^3 Å, the state density for angles of misfit $\Theta > 10^\circ$ is

[6] H. F. MATARÉ et al., Phys. Rev. **98**, 1179 [1955]; Z. Phys. **145**, 206 [1956].

[7] W. T. REED, Philosoph. Magazine **45**, 775, 119 [1954]; **46**, 111 [1955].

$N_a \approx 8 \cdot 10^{14}$ to 10^{16} cm^{-3}. With these states strongly localized, the FERMI level may fall into the valence band. At lower temperatures where the impurities become deionized, the boundary of the overlapping space charge cylinders becomes more and more defined, and the net space charge density

$$\varrho = q(N_d - N_a - n + p) \tag{3}$$

becomes $\varrho \approx q(p-n)$.

p, n = excess carries density (holes and electrons).

For a medium angle boundary, the filling factor will not be defined in the same manner as for isolated edge-dislocation pipes. If a planar space charge region results, due to overlapping space charge cylinders also in a direction perpendicular to the tilt axis, one will have a dependence of the number of available states on the cross voltage V_a applied:

$$f = \frac{1}{2}\left[1 + \left(1 + \frac{e V_a}{\Phi}\right)^{1/2}\right] \text{(see note [1])} \tag{4}$$

here: Φ work function, V_a applied voltage, $V_a = V_2 - V_1$ voltage difference at both grain boundary sides, e electron charge.

With voltages up to 100 volts applied to bicrystal interfaces, the number of electrons per site can thus increase to values $f > 1$. The space charge cylinders, therefore, will increase for this factor.

Appendix

If the SCHOTTKY barrier layer current voltage equation:

$$i_e = \frac{e \mu_e E [n_e - n_{e0} \exp(-e V_1/k T)]}{[1 - \exp(-e V_1/k T)]} \tag{5}$$

is applied to both boundary sides for the equilibrium case $[i_e(V_1) = i_e(V_2)]$ the dependence of the electron density on the dangling bond levels takes a form:

$$\frac{\partial n_e}{\partial V_a} = \frac{n_{e0}}{q}\frac{e}{k T}\left[V_2^{1/2}\left(\frac{k T}{2 e V_2} - 1\right)\frac{\partial V_2}{\partial V_a}\exp\left(-\frac{e V_2}{k T}\right) - V_1^{1/2}\left(\frac{k T}{2 e V_1} - 1\right)\frac{\partial V_1}{\partial V_a}\exp\left(-\frac{e V_1}{k T}\right)\right] \tag{6}$$

(compare note [6]) with the usual notations.

For the conditions: $V_2 \gg k T/e$ and $V_1 \gg k T/e$, (6) is a positive function with V_a increasing. This indicates strong filling of the free bonds with increasing V_a . Introducing now the filling factor (4), one gets:

$$n_e(q) = n_{e0}\frac{2}{q_0[1 + (1 + e V_a/\Phi)^{1/2}]} \cdot \left[V_2^{1/2}\exp\left(-\frac{e V_2}{k T}\right) - V_1^{1/2}\exp\left(-\frac{e V_1}{k T}\right)\right] \tag{7}$$

(n_{e0} equilibrium number for $V_a = 0$)
an expression for the electron density.

The change in the number of boundary states with a change in voltage V_a is then:

$$\frac{\partial n_e(q)}{\partial V_a} = \frac{2 n_{e0}}{q_0}\cdot\frac{1}{1 + (1 + e V_a/\Phi)^{1/2}}\left\{V_2^{1/2}\left(\frac{1}{2 V_2} - \frac{e}{k T}\right)\frac{\partial V_2}{\partial V_a}\exp\left(-\frac{e V_2}{k T}\right) - V_1^{1/2}\left(\frac{1}{2 V_1} - \frac{e}{k T}\right)\frac{\partial V_1}{\partial V_a}\exp\left(-\frac{e V_1}{k T}\right) + \frac{1}{1 + (1 + e V_a/\Phi)^{1/2}}\frac{e/\Phi}{2(1 + e V_a/\Phi)^{1/2}}\left[V_1^{1/2}\exp\left(-\frac{e V_1}{k T}\right) - V_2^{1/2}\exp\left(-\frac{e V_1}{k T}\right)\right]\right\} \tag{8}$$

which for the conditions:

$$e V_a \gg \Phi, \quad e V_1 \gg k T, \quad V_1 \gg V_2$$

degenerates to:

$$\frac{\partial n_e(q)}{\partial V_a} = \frac{2 n_{e0}}{q}\sqrt{\frac{\Phi}{e V_a}}\; V_2^{1/2}\exp\left(-\frac{e V_2}{k T}\right)\left[\left(\frac{1}{2 V_2} - \frac{e}{k T}\right)\frac{\partial V_2}{\partial V_a} + \frac{1}{2 V_a}\right]. \tag{9}$$

This equation shows that the change of the carrier density with applied voltage at the grain boundary is strong (positive with V_a increasing), but levels off for rather small voltages V_a .

As explained earlier [6], the high sensitivity of the grain boundary regions to potential changes across the barrier (ohmic or injecting contacts) is due to an accumulation of carriers in excited states, i. e. holes in hydrogenic states around shared electrons, in this region of high mechanical energy, (band gap change). Since we showed that there is a strong dependence of the number of sites from the cross voltage V_a applied to the grain boundary, there is, therefore, also a strong dependence of the sheet conductivity on the field across the SCHOTTKY barrier at either side.

The authors wish to thank C. TUFTS for electron-microscopic studies on grain boundaries. (Fig. 2.)